Journal of
Mechanical
Science and
Technology

Journal of Mechanical Science and Technology 21 (2007) 1226~1234

Analytical Method of Beat Tuning in a Slightly Asymmetric Ring

H. G. Park[a], S. H. Kim[b], Y. J. Kang[a,*]

[a]*School of Mechanical and Aerospace Engineering, Seoul National University, San 56-1, Shinlim-dong Kwanak-gu, Seoul 151-742 301-215*
[b]*Division of Mechanical Engineering and Mechatronics, Kangwon National University*

(Manuscript Received March 2, 2007; Revised April 2, 2007; Accepted June 1, 2007)

Abstract

In this research, we propose an analytical method to control the period and the clarity of the beat in a slightly asymmetric ring. The concept of a simple equivalent ring is applied, i.e. a slightly asymmetric ring with known modal data is modeled as an equivalent circular ring with one or multiple point masses, which has the same modal data as that of the original ring. By using the equivalent ring model, the optimal beat tuning is achieved by adding a 2nd point mass in order to obtain the required period and clarity in the beating vibration. The results obtained from the analytical method are compared with those obtained from finite element analysis(FEA) and the validity of the proposed method is verified. The proposed method can be effectively used to predict the mode pair and control the beat property in bell-type structures.

Keywords: Asymmetric ring; Beat tuning

1. Introduction

The circular ring model has been widely used for the analysis of the axisymmetric cylindrical structure. In this case, the circular ring is asymmetry because of the local stiffness or thickness deviation : this asymmetry is significantly different from other axisymmetric structures in terms of the vibration characteristics. Due to slight asymmetry, a frequency and mode pair appears and this causes a beat, which is a very interesting vibration characteristic. For the application cases, research was carried out on a bell-type structure(kim et al., 1994; Yum, 1984), tire (Allaei et al., 1988) and gyro ring. Allei and Soedel applied the receptance method to calculate the mode pair of the circular ring with local masses and springs(Kim et al., 1994; Allaei et al., 1998). Using the Rayleigh-Ritz method, Fox analyzed the modal parameters of a circular ring with multiple point masses and introduced the concept of an equivalent imperfection mass. He applied the analysis to reduce or eliminate the frequency split in a slightly asymmetric ring(Fox et al., 1990 ; Rourke et al., 2001). Hong and Lee analyzed an asymmetric circular ring and then obtained a precise solution considering the local mass and stiffness deviations as a heavy side step function(Hong and Lee, 1994). On the other hand, Kim et al. have investigated the beat distribution characteristics by using the impulse response model of a light asymmetric ring(Kim et al., 2005 ; Lee et al., 2002). There are many researches theoretically analyzing the mode characteristics of an asymmetric circular ring; however, there are very few researches on creating an equivalent circular ring, which has the required mode characteristics and vice versa. In this research, we suggest a method for creating a circular ring with asymmetry that satisfies the required beat condition for the purpose of application to a bell-type structure. Asymmetry is

*Corresponding author. Tel.: +82 2 880 1691, Fax.: +82 2 883 1513
E-mail address: yeonjune@snu.ac.kr

inevitably caused in casting or is designed intentionally in a bell-type structure. As a result, the beat phenomenon that repeats the strong and weak vibrations appears and this is an important characteristic of the Korean bell sound. However, it is difficult to generate a clear beat with a proper period. In this research, we suggest a new analytical method that consists of an asymmetric circular ring with the required beat and mode pair characteristics. Fox applied a simple equivalent ring model to eliminate the beat. However, in a Korean bell, a clear beat with a proper period is required. In order to apply Fox's method for tuning the beat, we should improve upon his theory and check in detail the position and magnitude of the 2nd mass that is attached.

First, we prove theoretically that the mode characteristics of both the models vary equally when we add a 2nd point mass to the original model and its simple equivalent model. Based on this theory, we expect an alterlation in the mode pair and natural frequencies due to the attachment of the 2nd point mass to the simple equivalent model whose mode characteristics are known. Moreover, we suggest a new method to determine the position of the optimal 2nd point mass for the required beat condition. We use the impulse response model of a slightly asymmetric circular ring in order to analyze the clarity of the beat and verify the reliability by a comparison between the theoretical and finite element analysis(FEA) results.

2. Theory for the equivalent ring model

We assume that the beat frequencies and mode shapes of the circular ring are obtained from the measurement in which the magnitude and position of the imperfection masses are not known. In other words, the natural frequency pair $\omega_{L,H}$, the phase of the mode pair $\psi_{L,H}$ and the total mass of the circular ring M are provided. We use Fox's model since it is easy to obtain a simple equivalent ring model with the same mode characteristics. Fox proposed a theoretical model of a slightly asymmetric ring with multiple point masses using the Rayleigh-Ritz method. He derived the following Eqs. for the natural frequencies and the node position of the circumferential modes(Rurke et al., 2001). These Eqs. imply that if we know the magnitude and location of the imperfection masses, we can obtain the natural frequencies and the node positions of the circular ring with multiple point masses.

$$\tan 2n\psi_n = \frac{\sum_i m_i \sin 2n\phi_i}{\sum_i m_i \cos 2n\phi_i} \tag{1}$$

$$\omega_{nL,H}^2 = \omega_{0n}^2 \left(\frac{1+\alpha_n^2}{(1+\alpha_n^2)+\sum_i m_i[(1+\alpha_n^2)\mp(1-\alpha_n^2)\cos 2n(\phi_i-\psi_n)]/M_0} \right) \tag{2}$$

(n : mode number, m_i : i-th point mass, ϕ_i : position of i-th point mass, ψ_n : node of n-th mode, α_n : ratio of radial displacement to tangential displacement, M_0 : mass of perfect circular ring)

We consider a circular ring with n imperfection point masses that satisfy the mode characteristics, $\omega_{nL,nH}$ and ψ_n, and can transform Eqs. (1) and (2) to Eqs. (3) and (4), respectively, by using standard trigonometric identities.

$$\sum m_i \sin 2n(\phi_i - \psi_n) = 0 \tag{3}$$

$$\sum m_i \cos 2n(\phi_i - \psi_n) = M\lambda_n,$$

$$\lambda_n = \frac{(\omega_{nL}^2 - \omega_{nH}^2)(1+\alpha_n^2)}{(\omega_{nL}^2 + \omega_{nH}^2)(1-\alpha_n^2)}, \tag{4}$$

$$M = M_0 + \sum m_i = M^* + m_{eq}$$

The simple equivalent model with an imperfection point mass is obtained from the condition that the nth mode satisfies the given mode data $\omega_{nL,nH}$ and ψ_n. If we consider a point mass m_{eq}, the following Eqs. are introduced from the Eqs. (3) and (4).

$$m_{eq} \sin 2n(\phi_{eq} - \psi_n) = 0 \;\Rightarrow\; \phi_{eq} = \psi_n + \frac{\pi}{2n} \tag{5}$$

$$m_{eq} \cos 2n(\phi_{eq} - \psi_n) = M\lambda_n \;\Rightarrow\; m_{eq} = M\lambda_n \tag{6}$$

Therefore, we can obtain the simple equivalent circular ring model with the same mode data as that of the original ring if we attach the mass $m_{eq} = M\lambda_n$ to the position $\phi_{eq} = \psi_n + \frac{\pi}{2n}$.

3. Validity of the equivalent ring model

The simple equivalent circular ring model should have the same mode characteristics as those of the original ring; further, it should have the same

variation with the original ring in terms of the natural frequency and mode shape in the case of structure modifications. Here, we theoretically check whether the mode characteristics of both the models change equally when we add a new mass m_{new} to the position ϕ_{new} in both the models. As an initial asymmetric ring, we consider a circular ring with multiple point masses satisfying Eqs. (1) and (2), and we develop another circular ring model with a point mass using Eqs. (5) and (6), which has the same mode data as those of the initial model. If we add a new mass m_{new} to the position ϕ_{new} in both the models, the anti-node of the L-mode ψ_n is determined by using Eqs. (7) and (8).

$$\tan 2n\psi_n = \frac{\sum_i m_i \sin 2n\phi_i}{\sum_i m_i \cos 2n\phi_i} = \frac{m_{eq} \sin 2n\phi_{eq}}{m_{eq} \cos 2n\phi_{eq}} \tag{7}$$

$$\tan 2n\psi_n' = \frac{\sum_i m_i \sin 2n\phi_i + m_{new} \sin 2n\phi_{new}}{\sum_i m_i \cos 2n\phi_i + m_{new} \cos 2n\phi_{new}} \tag{8}$$

$$\tan 2n\psi_n'' = \frac{m_{eq} \sin 2n\phi_{eq} + m_{new} \sin 2n\phi_{new}}{m_{eq} \cos 2n\phi_{eq} + m_{new} \cos 2n\phi_{new}} \tag{9}$$

Here, the combination of the Eqs (4) and (6) gives Eq. (10).

$$m_{eq} = M\lambda_n = \sum m_i \cos 2n(\phi_i - \psi_n) \tag{10}$$

From Eq. (5), we know that ϕ_{eq} is equal to ψ_n. Multiplying $\cos 2n\phi_{eq}$ with Eq. (10) gives

$$\begin{aligned} m_{eq} \cos 2n\phi_{eq} &= \cos 2n\psi_n \sum m_i \cos 2n(\phi_i - \psi_n) \\ &= \frac{1}{2} \sum m_i \left[\cos 2n\phi_i + \cos 2n(\phi_i - 2\psi_n) \right] \end{aligned} \tag{11}$$

Further, multiplying $\sin 2n\psi_n$ with Eq. (3) gives

$$\begin{aligned} &\sin 2n\psi_n \times \sum m_i \sin 2n(\phi_i - \psi_n) \\ &= \frac{1}{2} \sum m_i \left[-\cos 2n\phi_i + \cos 2n(\phi_i - 2\psi_n) \right] \\ &= 0 \end{aligned} \tag{12}$$

As a result, Eq. (13) is obtained as follows.

$$\frac{1}{2} \sum m_i \cos 2n(\phi_i - 2\psi_n) = \frac{1}{2} \sum m_i \cos 2n\phi_i \tag{13}$$

By substituting Eq. (13) in Eq. (11), we obtain

$$m_{eq} \cos 2n\phi_{eq} = \sum m_i \cos 2n\phi_i \tag{14}$$

Further, the combination of Eqs. (7) and (14) shows that

$$\begin{aligned} &m_{eq} \cos 2n\phi_{eq} = \sum m_i \cos 2n\phi_i \quad \Rightarrow \\ &m_{eq} \sin 2n\phi_{eq} = \sum m_i \sin 2n\phi_i \end{aligned} \tag{15}$$

Likewise, by equating Eqs. (15), (8) and (9), we show that

$$\begin{aligned} \tan 4\psi_1' = \tan 4\psi_1'' &= \frac{\sum_i m_i \sin 4\phi_i + m_{new} \sin 4\phi_{new}}{\sum_i m_i \cos 4\phi_i + m_{new} \cos 4\phi_{new}} \\ &= \frac{m_{eq} \sin 4\phi_{eq} + m_{new} \sin 4\phi_{new}}{m_{eq} \cos 4\phi_{eq} + m_{new} \cos 4\phi_{new}} \end{aligned} \tag{16}$$

As a result, we prove that ψ_1' is equal to ψ_1''.

Besides, the new natural frequencies $\omega_{nL,nH}'$ and $\omega_{nL,nH}''$ are calculated as follows:

$$M = M_0 + \sum_{i=1}^{n} m_i = M^* + m_{new}$$

$$\begin{aligned} \omega_{nL,nH}'^2 &= \omega_{0n}^2 \left(\frac{1 + \dfrac{\alpha_n^2}{/M_0 + m_{new}[(1+\alpha_n^2) \mp (1-\alpha_n^2)\cos 2n(\phi_{new} - \psi_n')]/M_0}}{(1+\alpha_n^2) + \sum_{i=1}^{n} m_i[(1+\alpha_n^2) \mp (1-\alpha_n^2)\cos 2n(\phi_i - \psi_n')]} \right) \end{aligned} \tag{17}$$

$$\begin{aligned} \omega_{nL,nH}''^2 &= \omega_{0n}^{*2} \left(\frac{1 + \dfrac{\alpha_n^2}{/M^* + m_{new}[(1+\alpha_n^2) \mp (1-\alpha_n^2)\cos 2n(\phi_{new} - \psi_n'')]/M^*}}{(1+\alpha_n^2) + m_{eq}[(1+\alpha_n^2) \mp (1-\alpha_n^2)\cos 2n(\phi_{eq} - \psi_n'')]} \right) \end{aligned} \tag{18}$$

Eqs. (19) and (20) are derived from Eqs. (3) and (5) before we add a new mass m_{new}.

$$\begin{aligned}
&\sum m_i \sin 2n(\phi_i - \psi_n)\sin 2n(\psi_n - \psi_n') = 0 \\
&= \frac{1}{2}\sum m_i[-\cos 2n(\phi_i - \psi_n + \psi_n - \psi_n') \\
&\qquad + \cos 2n(\phi_i - \psi_n - \psi_n + \psi_n') \\
&= \frac{1}{2}\sum m_i[-\cos 2n(\phi_i - \psi_n') \\
&\qquad + \cos 2n(\phi_i - 2\psi_n + \psi_n') = 0 \\
&\therefore \sum m_i \cos 2n(\phi_i - \psi_n') \\
&\quad = \sum m_i \cos 2n(\phi_i - 2\psi_n + \psi_n')
\end{aligned} \tag{19}$$

$$\begin{aligned}
&m_{eq} \sin 2n(\phi_{eq} - \psi_n)\sin 2n(\psi_n - \psi_n') = 0 \\
&= \frac{1}{2}\Big[-m_{eq} \cos 2n(\phi_{eq} - \psi_n + \psi_n - \psi_n') \\
&\quad + m_{eq} \cos 2n(\phi_{eq} - \psi_n - \psi_n + \psi_n')\Big] \\
&\therefore m_{eq} \cos 2n(\phi_{eq} - \psi_n') \\
&\quad = m_{eq} \cos 2n(\phi_{eq} - 2\psi_n + \psi_n')
\end{aligned} \tag{20}$$

Likewise, Eqs. (21) and (22) are derived from Eqs. (4) and (6).

$$\sum m_i \cos 2n(\phi_i - \psi_n) = m_{eq} \cos 2n(\phi_{eq} - \psi_n) = M\lambda_n \tag{21}$$

$$\begin{aligned}
&\sum m_i \cos 2n(\phi_i - \psi_n)\cos 2n(\psi_n - \psi_n') \\
&\quad = m_{eq} \cos 2n(\phi_{eq} - \psi_n)\cos 2n(\psi_n - \psi_n') \\
&\sum m_i \cos 2n(\phi_i - \psi_n') \\
&\quad + \sum m_i \cos 2n(\phi_i - 2\psi_n + \psi_n') \\
&\quad = m_{eq} \cos 2n(\phi_{eq} - \psi_n') \\
&\quad + m_{eq} \cos 2n(\phi_{eq} - 2\psi_n + \psi_n')
\end{aligned} \tag{22}$$

If we substitute Eqs. (19) and (20) in Eq. (22), Eq. (23) is obtained.

$$\sum m_i \cos 2n(\phi_i - \psi_n') = m_{eq} \cos 2n(\phi_{eq} - \psi_n') \tag{23}$$

Equating Eqs. (23), (17), and (18) shows that

$$\begin{aligned}
&\omega_{nL,nH}'^2 \\
&= \frac{1+\alpha_n^2}{\frac{1}{\omega_{0n}^2}(1+\alpha_n^2) + \frac{1}{\omega_{0n}^2 M_0}\Big[\sum m_i(1+\alpha_n^2) \mp m_{eq}(1-\alpha_n^2)\cos 2n(\phi_{eq} - \psi_n')\Big]} \\
&\quad + \frac{m_{new}}{\omega_{0n}^2 M_0}[(1+\alpha_n^2) \mp (1-\alpha_n^2)\cos 2n(\phi_{new} - \psi_n')] \\
&= \frac{1+\alpha_n^2}{\frac{1}{\omega_{0n}^2 M_0}\Big(M_0 + \sum m_i\Big)(1+\alpha_n^2) \mp \frac{1}{\omega_{0n}^2 M_0} m_{eq}(1-\alpha_n^2)\cos 2n(\phi_{eq} - \psi_n')} \\
&\quad + \frac{m_{new}}{\omega_{0n}^2 M_0}[(1+\alpha_n^2) \mp (1-\alpha_n^2)\cos 2n(\phi_{new} - \psi_n')]
\end{aligned} \tag{24}$$

and

$$\begin{aligned}
&\omega_{nL,nH}^{*2} \\
&= \frac{1+\alpha_n^2}{\frac{1}{\omega_{0n}^{*2}}(1+\alpha_n^2) + \frac{1}{\omega_{0n}^{*2} M^*} m_{eq}[(1+\alpha_n^2) \mp (1-\alpha_n^2)\cos 2n(\phi_{eq} - \psi_n^*)]} \\
&\quad + \frac{m_{new}}{\omega_{0n}^{*2} M^*}[(1+\alpha_n^2) \mp (1-\alpha_n^2)\cos 2n(\phi_{new} - \psi_n^*)] \\
&= \frac{1+\alpha_n^2}{\frac{1}{\omega_{0n}^{*2} M^*}(M^* + m_{eq})(1+\alpha_n^2) \mp \frac{1}{\omega_{0n}^{*2} M^*} m_{eq}(1-\alpha_n^2)\cos 2n(\phi_{eq} - \psi_n^*)]} \\
&\quad + \frac{m_{new}}{\omega_{0n}^{*2} M^*}[(1+\alpha_n^2) \mp (1-\alpha_n^2)\cos 2n(\phi_{new} - \psi_n^*)]
\end{aligned} \tag{25}$$

Here, the radius of the circular ring R and the thickness h are fixed and Eq. (26) is derived.

$$\begin{aligned}
\omega_{0n}^2 M_0 &= \omega_{0n}^{*2} M^* \\
&= \frac{1}{R^2}\frac{E}{\rho(1-\nu^2)}\frac{(n-\alpha_n)^2 + \beta\alpha_n^2(1-n^2)^2}{1+\alpha_n^2} \\
&\quad \left[\left(R + \frac{h}{2}\right)^2 - \left(R - \frac{h}{2}\right)^2\right]\pi d\rho \\
&= \frac{E}{R}\frac{2h\pi d}{(1-\nu^2)}\frac{(n-\alpha_n)^2 + \beta\alpha_n^2(1-n^2)^2}{1+\alpha_n^2}
\end{aligned} \tag{26}$$

If we substitute Eqs. (4) and (26) in Eqs. (24) and (26), Eq. (27) is obtained.

$$\begin{aligned}
&\omega_{nL,nH}'^2 = \omega_{nL,nH}^{*2} \\
&= \frac{1+\alpha_n^2}{\frac{1}{\omega_{0n}^2 M_0}\Big(M_0 + \sum m_i\Big)(1+\alpha_n^2) \mp \frac{1}{\omega_{0n}^2 M_0} m_{eq}(1-\alpha_n^2)\cos 2n(\phi_{eq} - \psi_n')} \\
&\quad + \frac{m_{new}}{\omega_{0n}^2 M_0}[(1+\alpha_n^2) \mp (1-\alpha_n^2)\cos 2n(\phi_{new} - \psi_n')] \\
&= \frac{1+\alpha_n^2}{\frac{1}{\omega_{0n}^{*2} M^*}(M^* + m_{eq})(1+\alpha_n^2) \mp \frac{1}{\omega_{0n}^{*2} M^*} m_{eq}(1-\alpha_n^2)\cos 2n(\phi_{eq} - \psi_n^*)]} \\
&\quad + \frac{m_{new}}{\omega_{0n}^{*2} M^*}[(1+\alpha_n^2) \mp (1-\alpha_n^2)\cos 2n(\phi_{new} - \psi_n^*)]
\end{aligned} \tag{27}$$

In conclusion, we know that the simple equivalent model, which has the same mode characteristics as those of the initial model with multiple point masses is founded to be unique and the variation in the natural frequencies and mode shapes of both the

models coincide exactly, regardless of the number and position of the masses of the initial model.

4. Analysis of the equivalent ring model

Table 1 shows the specifications of the circular ring, which are determined to have the same frequency of the n=2 mode as that of the famous King Seongdeok Divine Bell(Kim et al., 2005). With the symmetric ring, we generate asymmetry using five point masses; m_i=[3, 1, 4, 6, 4]kg, Φ_i=[0, 35, 125, 260, 300]°. As a result, the original asymmetric ring model is created and has mode data as given in Table 1. We assume we do not know the magnitude and position of the imperfection masses; we start tuning simulation only with the original modal data. From the mode characteristics, we can obtain the n=2 and n=3 simple equivalent models with a point mass that satisfies the mode characteristics for both the n=2 and n=3 modes using Eqs. (5) and (6).

Modal data of the original model : M=1702.5 kg, $\omega_{2L}=64.57$ Hz, $\omega_{2H}=64.64$ Hz, $\phi_2=14.49°$, $\omega_{3L}=182.25$ Hz, $\omega_{3H}=183.05$ Hz, $\phi_3=7.57°$

n=2 equivalent model : m_1=[3.3285]kg, Φ_1=[14.49]°

n=3 equivalent model : m_1=[9.4143]kg, Φ_1=[7.57]°

In Table 1, ω_0 is the natural frequency of the symmetric ring without point masses and it does not show a mode split. As theoretically verified, only in the n=2 mode, the frequency and phase of the n=2 equivalent model are exactly the same as those of the original ring with five point masses: an identical situation is observed in the n=3 equivalent model as shown in the table.

Figure 1 shows the mode condition of the n=2 and n=3 modes between the original model and the equivalent model. The mode pairs of both the models coincide, as confirmed theoretically. In Fig. 1, the anti-node of the L-mode becomes the node of the H-mode; therefore, the mode shapes can be expressed by only the anti-node of the L-mode. When we compare the n=2 equivalent model with the original model, the mode shapes of n=2 mode coincide but to the ratio of m_{eq} to M using the FEA results. As expec- ted those of the n=3 mode do not coincide. Likewise, in the case of the n=3 equivalent model, the mode shapes of the n=3 mode only coincide with each other. In other words, the equivalent model with a point mass follows only a target mode in the mode characteristics.

Table 1. Natural frequency of original ring and equivalent rings.

Specification of axisymmetric ring	M=1702.5 kg, ρ=8700 kg/m³, R=1.012 m, E=5.6e10 Pa, h=0.203 m, d=0.15 m			
Mode parameter	Mode	ω_1	ω_2	Φ_1
Original	n=2	64.57	64.64	14.49
	n=3	182.25	183.05	7.57
n=2 equivalent model	n=2	64.57	64.64	14.49
	n=3	182.50	182.79	14.49
n=3 equivalent model	n=2	64.50	64.71	7.57
	n=3	182.25	183.05	7.57

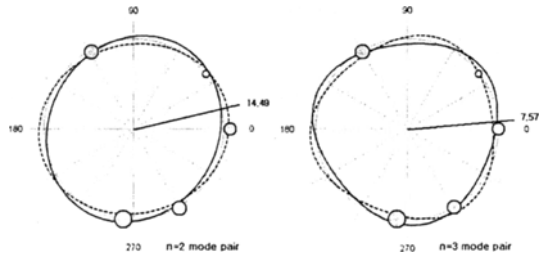

(a) Original ring model with 5-masses

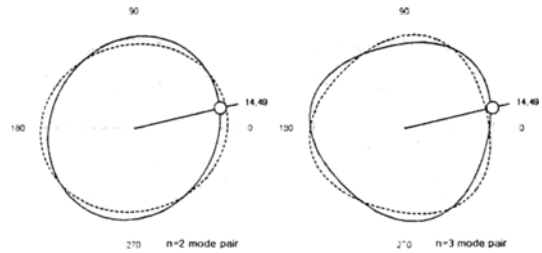

(b) n=2 equivalent ring model with a point mass

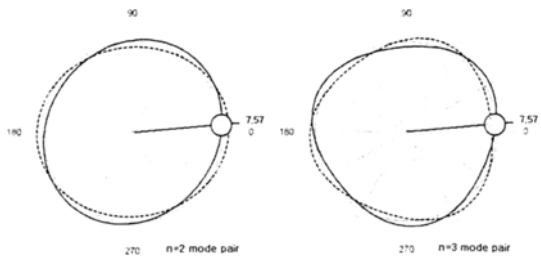

(c) n=3 equivalent ring model with a point mass

Fig. 1. Original ring and equivalent models.

In Fig. 2, we compare the frequency pair according expected, as the ratio of m_{eq} to M increase, a difference between the frequencies occurs and the difference in the frequency pair(beat frequency) increases. The difference in the frequencies in the comparison between the FEA results and the theoretical results, is because the ratio of the thickness to

the radius of the ring is comparatively large. However, we focus on the changing tendency of the frequency and mode pairs, and the characteristics of both the models are very similar.

Figure 3(a) shows the magnitude of the frequency pair according to the location of the 2nd point mass which has the same magnitude(m_{eq}/M=0.002) as that of the 1st imperfection point mass of the equivalent model. An imperfection point mass of the equivalent model is located at the position corresponding to 14.49° as shown in Fig. 1(b). The initial asymmetry can increase or decrease according to the position of the 2nd point mass. If we attach the 2nd point mass to a location that is shifted 45°(Φ_{2nd} = 59.49°) from the 1st point mass, the effect of asymmetry becomes zero and the frequencies of the L-mode and H-mode become equal. If we attach the 2nd point mass to a location that is shifted 90° from 54.59°, the same effects are observed. These results agree with those of the beat trimming by Fox. On the contrary, if we attach the 2nd point mass to the same position as that of the 1st mass or if the location is shifted 90° from that position, the effect of asymmetry and the difference in the frequency pair reaches the maximum.

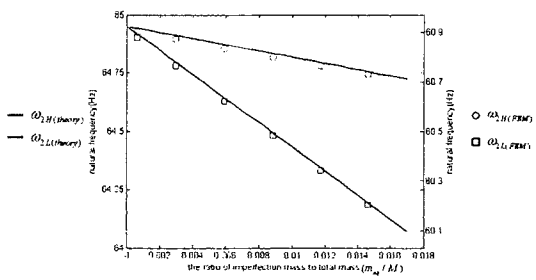

Fig. 2. Frequency vs. the ratio of imperfection mass to total mass

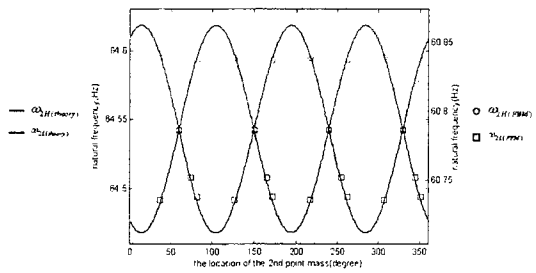

(a) Frequency vs. the location of 2nd point mass

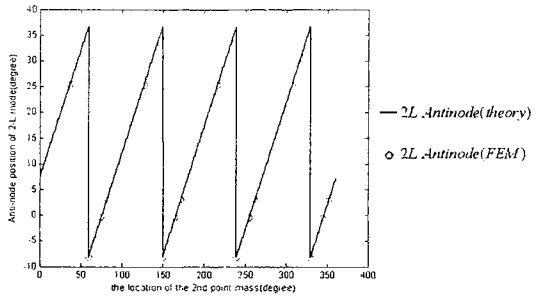

(b) Anti-node position of n=2 L-mode vs. point mass position

Fig. 3. Change of mode data by a point mass attachment.

Figure 3(b) shows the anti-node of the L-mode according to the position of the 2nd point mass. The positions of the mode and anti-node are very important in tuning the beat response of the asymmetric circular ring. The position of the n=2 anti-node has a period and the variation of the n=2 anti-node position by the 2nd point mass also has a period. The discontinuity in the Φ_{2nd} = 59.49° position means that the mode separation does not occur due to the cancellation effect of the 2nd point mass and this is periodically generated. The theoretical results of Figs. 3(a) and (b) are in complete agreement with the FEA results.

Figure 4 shows the natural frequency and the node position according to the magnitude and position of the 2nd point mass. The final objective of our research is to control the beat(inverse of the difference between the low and high frequencies) and node position based on our intent.

Figure 4(a) represents the variation of the beat due to the magnitude of the 2nd point mass, which is 1/4, 1/2, 1, 2 and 4 times the initial mass. As stated previously, when we add a 2nd mass to the Φ_{2nd}= 59.49° position, the beat period becomes maximum irrespective of the magnitude of the 2nd mass. This means that the amount of asymmetry reaches the minimum when we attach a 2nd mass to a position that is shifted 45° from the 1st mass. In particular, when the magnitude of the 2nd point mass is the same as that of the 1st mass, the beat period becomes infinite and the beat is eliminated. The beat period increases as the 2nd point mass approaches to the 1st mass in both case that 2nd point mass is bigger or less than the 1st mass. The reason is that the attachment of the 2nd point mass produces a cancellation effect of the asymmetry. However, the asymmetry reaches the maximum while the beat period reaches the minimum when we add a 2nd point mass to the Φ_{2nd}=14.49° position because this position is the same as that of the 1st mass in the initial equivalent model. As the 2nd point mass increases, the amount of asymmetry increases and the beat period decreases. These tendency repeat within

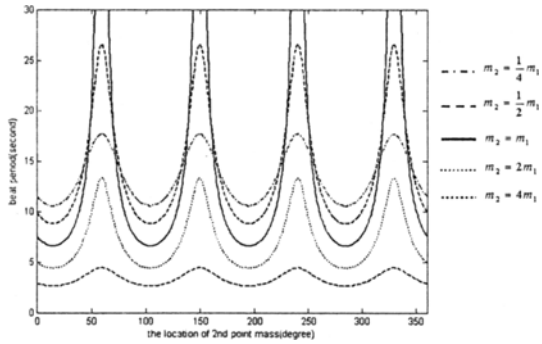

(a) Beat period vs. 2_{nd} mass position

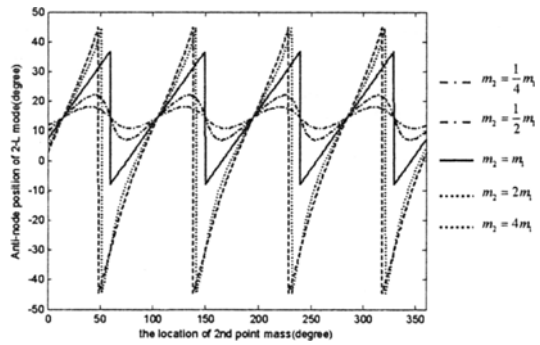

(b) Node position vs. 2_{nd} mass position

Fig. 4. Change of mode pair by the attachment of 2_{nd} point mass.

acircle of 90°. If the amount of initial asymmetry is different, the maximum and minimum points on the curved line change; however, the configuration of the n=2 mode curved lines is identical. Applying the same analytical method, we can draw n=3 mode curved lines and expect a variation of the beat frequencies. Figure 4(b) shows the location of the L-mode anti-node according to that of the attached 2nd mass. When we add a 2nd point mass to the position corresponding 14.49° which is the same as that of the 1st mass, or the position that is shifted 90° from 14.49°, the anti-node of the L-mode(the node of the H-mode) does not shift from the initial location, i.e., 14.49°. The attachment of the 2nd mass to these positions causes an increase in the mass effect of the L-mode and maintains the phase of the L-mode. On the other hand, a rapid transition appears at the position corresponding 59.49°, which is a 90° shift from the position of the 1st mass, and these characteristics repeat within a circle of 90°. It is very important to consider these points when we attempt to move the nodal line for generating a clear beat. In this manner, we expect a variation of the natural frequencies and node position and find an effective method for the structure modification in order to satisfy the required mode characteristics from a simple equivalent model. This equivalent model can be applied to obtain the alteration of the mode characteristics for higher modes as well(n=3, 4,...).

5. Beat tunning for clearness and proper period

In Korean bell, a clear beat with a proper period is required. The clarity of the beat can be analyzed by the following impulse response model of a slightly asymmetric circular ring.(Kim et al., 2005)

$$\ddot{u}_{3n}(\theta,t) = -e^{-\zeta_{na}\frac{\omega_{nL}+\omega_{nH}}{2}t} [\cos n(\theta^* - \phi_L)\cos n(\theta - \phi_L)\sin(\omega_{nL}t) + \cos n(\theta^* - \phi_H)\cos n(\theta - \phi_H)\sin(\omega_{nH}t)] \quad (28)$$

(ζ_{na} : average value of damping, ω_{nH} : natural frequency of a high mode, ω_{nL} : natural frequency of a low mode, θ^* : position of the striking point, ϕ_L : position of the anti-node of low mode, ϕ_H : position of the anti-node of high mode)

The striking point is fixed at the design stage in a bell-type structure. From Eq. (28), the low and high mode pairs should be equally excited for a clear beat. Therefore, each anti-node of the mode pairs should be positioned at an equal distance from the striking point. This requires the anti-node of the n=2 L-mode to be positioned 22.5° from the striking point. By substituting $\phi_2 = 22.5°$ in Eq. (2), we can obtain the condition of the 2nd mass m_2 and position ϕ_2, i.e., it is determined how much and what position the 2nd mass should be attached to in order to make the anti-node of the L-mode shift to 22.5°. The solid line in Fig. 5(a) represents this condition. Positive mass refers to the attachment of the mass and negative mass refers to the removal of the mass. An infinite amount of the 2nd point mass is required at 22.5° or 67.5° for the L-mode anti-node to be located exactly at 22.5°. At the 45° position, the same result can be obtained with minimum 2nd mass attachment. Therefore, for the present asymmetric ring, a 45° position (or its 90° periodic positions) will be the optimal position with respect to the clarity of the beat. However, the optimal position will vary according to the initial asymmetry of the original ring. Both the

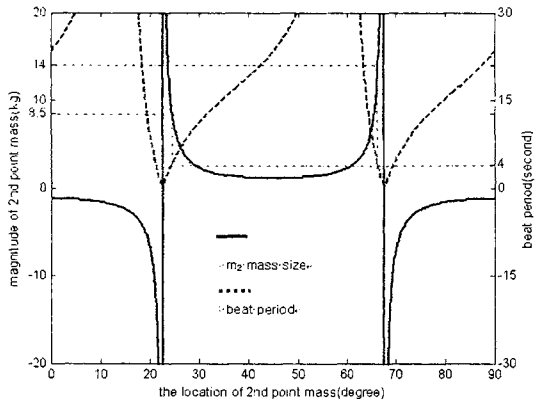

Fig. 5. 2nd mass size and beat period vs. 2nd mass position.

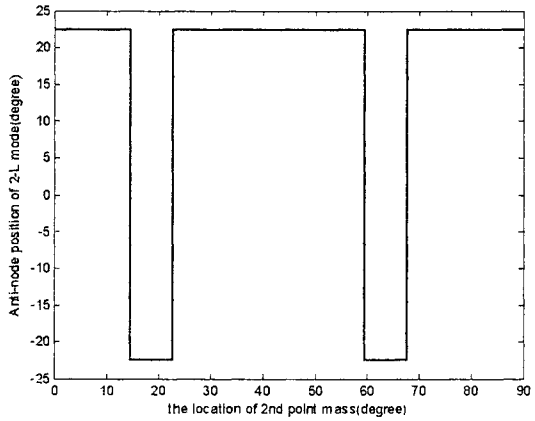

Fig. 6. L-mode anti-node position vs. 2nd mass position.

Table 2. Description of the considered circular ring after tuning.

Description of the circular ring	M=1711 kg, ρ=8700 kg/m³, R=1.012 m, E=5.6e10 Pa, h=0.203 m, d=0.15 m, m_i=[3.3285, 8.5]kg, Φ_i=[14.49, 25.45]			
Mode	ω_1	ω_2	ψ	Beat period
N=2	64.3206	64.5708	22.5	4
N=3	181.7566	182.6272	-7.4	1.15

period and clarity are important factors in the beat vibration. The dotted line in Fig. 5(a) represents the beat period(T: inverse of the beat frequency). This dotted line is obtained by substituting the values of m_2 on the solid line in Eq. (2). In the given ring model, the initial beat period of the n=2 mode was 13.3 s, which seems to be very high. As an application, we attempt to shorten the period to 4 s, to hold a clear beat. During this period, a 2nd point mass of 8.5 kg(m_2/m_1=2.5, i.e., m_2/M=0.005) should be attached at 25.45°, as shown in Fig. 5(b). In this situation, the L-mode anti-node is located at -22.5° as shown in Fig. 5(b). Interestingly, a higher mass of 14 kg(m_2/M= 0.0082) is required at 65.7 degree for the same purpose.

Table 2 shows the beat tuning result. As expected, successful beat tuning is confirmed in the n=2 mode, i.e., the beat period becomes 4 s, and the L-mode anti-node is located at 22.5°. However, the result shows that the n=3 mode does not contribute to the beat tuning: this means that additional beat tuning is necessary for the n=3 mode.

In the proposed method, beat tuning is possible by using 2nd point mass. In reality it is more frequent to give cuts and modify the structure than to add masses. The cut simultaneously diminishes the mass and stiffness, and Hong(1990) showed that the stiffness reduction effect is considerably stronger than the mass reduction effect. Since the stiffness effect is much stronger than the mass effect, the anti-node of the L-mode passes the location of the cut; this result is the same as that obtained in the case of an equivalent mass located on the anti-node of the L-mode. This demonstrated possibility to some extent that the abovementioned theoretical analysis can be applied to the beat tuning method using the cut.

6. Conclusions

An equivalent ring model with a point mass was created, which has the same mode characteristics as that of a slightly asymmetric arbitrary circular ring. We theoretically proved that this equivalent ring has exactly the same natural frequencies and node positions for a specific mode pair and the variation of the mode characteristics by attaching a 2nd point mass coincides between both the models. An equivalent ring model is determined for each mode. We can intentionally control the location of the nodal line and the beat period of the mode pair. The theoretical results were compared with the FEA results and the reliability was verified. On the basis of the suggested analytical method, we can obtain the position of the mass that satisfies the required mode characteristics with a least 2nd point mass. In conclusion, the proposed beat tuning method using the equivalent ring model can be applied to effectively tune the beat characteristics of a bell-type structure.

References

Kim, S. H., Sodel, W. and Lee, J. M., 1994, "Analysis of the Beating Response of Bell Type Structures," *Journal of Sound and Vibration*, 173(4), pp. 517~536.

Allaei, D., Soedel W. and Yang, T. Y., 1988, "Vibration Analysis of Non-axisymmetric Tires," *Journal of Sound and Vibration*, 122, pp. 11~29.

Fox, C. H. J., 1990, "A Simple Theory for the Analysis and Correction of Frequency Splitting in Slightly Imperfect Rings," *Journal of Sound and Vibration*, 142(2), pp. 227~243.

Rourke, A. K., McWilliam, S. and Fox, C. H. J., 2001, "Multi-mode Trimming of Imperfect Rings", *Journal of Sound and Vibration*, 248(4), pp. 695~724.

Hong, J. S. and Lee, J. M., 1994, "Vibration of Circular Rings with Local Deviation," *Journal of Applied Mechanics*, 61, pp. 317~322.

Kim, S. H., Lee, C. W. and Lee, J. M., 2005, "Beat Characteristics and Beat Maps of the King Seong-deok Divine Bell," *Journal of Sound and Vibration*, 281, pp. 21~44.

Lee, J. M., Kim, S. H., Lee, S. J., Jeong, J. D. and Choi, H. G., 2002, "A Study on the Vibration Characteristics of a Large Size Korean Bell," *Journal of Sound and Vibration*, 257(4), pp. 779~790.

Yum, Y. H., 1984, "A Study on the Korean Bell," Research Institute of Korean Spirits and Culture Research Report 84-14.